

Laser-induced thermal lens study of the role of morphology and hydroxyl group in the evolution of thermal diffusivity of copper oxide

Riya Sebastian, M S Swapna, Vimal Raj, and S Sankararaman

Citation: Chin. Phys. B, 2021, 30 (**6**): 067801. DOI: 10.1088/1674-1056/abd9b5
Journal homepage: http://cpb.iphy.ac.cn; http://iopscience.iop.org/cpb

What follows is a list of articles you may be interested in

Effect of heating time on structural, morphology, optical, and photocatalytic properties of g-C_3N_4 nanosheets

Nguyen Manh Hung, Le Thi Mai Oanh, Lam Thi Hang, Pham Do Chung, Pham Thi Duyen, Dao Viet Thang, Nguyen Van Minh
Chin. Phys. B, 2020, 29 (**5**): 057801. DOI: 10.1088/1674-1056/ab7e95

Effects of deposition temperature on optical properties of MgF_2 over-coated Al mirrors in the VUV

Chun Guo(郭春), Bin-Cheng Li(李斌成), Ming-Dong Kong(孔明东), Da-Wei Lin(林大伟)
Chin. Phys. B, 2019, 28 (**11**): 117801. DOI: 10.1088/1674-1056/ab457a

SnS_2 quantum dots: Facile synthesis, properties, and applications in ultraviolet photodetector

Yao Li(李尧), Libin Tang(唐利斌), Rujie Li(李汝劼), Jinzhong Xiang(项金钟), Kar Seng Teng, Shu Ping Lau(刘树平)
Chin. Phys. B, 2019, 28 (**3**): 037801. DOI: 10.1088/1674-1056/28/3/037801

Recent research process on perovskite photodetectors:A review for photodetector – materials, physics, and applications

Yan Zhao(赵岩), Chenglong Li(李成龙), Liang Shen(沈亮)
Chin. Phys. B, 2018, 27 (**12**): 127806. DOI: 10.1088/1674-1056/27/12/127806

Spectral features and antibacterial properties of Cu-doped ZnO nanoparticles prepared by sol-gel method

Alireza Samavati, A F Ismail, Hadi Nur, Z Othaman, M K Mustafa
Chin. Phys. B, 2016, 25 (**7**): 077803. DOI: 10.1088/1674-1056/25/7/077803

Laser-induced thermal lens study of the role of morphology and hydroxyl group in the evolution of thermal diffusivity of copper oxide

Riya Sebastian, M S Swapna, Vimal Raj, and S Sankararaman†

Department of Optoelectronics, University of Kerala, Trivandrum 695581, *Kerala, India*

(Received 25 October 2020; revised manuscript received 6 January 2021; accepted manuscript online 8 January 2021)

The paper explores the evolution of thermal behavior of the material by studying the variations in thermal diffusivity using the single beam thermal lens (TL) technique. For this purpose, the decomposition of $Cu(OH)_2$ into CuO is studied in a time range up to 120 h, by subjecting the sample to morphological, structural, and spectroscopic characterizations. The time evolution of thermal diffusivity can be divided into three regions for demonstrating the dynamics of the reaction. When the reaction is complete, the thermal diffusivity is also found to be saturated. In addition to the morphological modifications, from rods to flakes, the variations in the amount of hydroxyl group are attributed to be responsible for the enhancement of base fluid's thermal diffusivity by 165%. Thus the study unveils the role of hydroxyl groups in the thermal behavior of CuO.

Keywords: thermal diffusivity, CuO, thermal lens, morphology, hydroxyl group

PACS: 78.20.nb, 66.30.Xj, 61.46.−w **DOI:** 10.1088/1674-1056/abd9b5

1. Introduction

The studies on nanomaterials of transition metal oxides are attractive because of their typical magnetic, electrical, and optical properties. Also, they show high thermal stability, hardness, and chemical resistance.[1] The oxide nanoparticles of the transition metals Ni, Zn, Fe, Ti, Co, Ce, and Cu are the commonly used materials for the preparation of nanofluids for heat transfer applications.[2–8] Copper oxide is one of the extensively investigated transition metal oxides for various applications ranging from the electronic industry to the chemical industry.[9–11] Copper oxide is a narrow bandgap metal oxide that possesses two different crystalline forms, named cuprous oxide (Cu_2O) and cupric oxide (CuO).[12] Cupric oxide shows good photovoltaic, catalytic, and electrochemical properties.[13,14] The nanoparticles of CuO have a wide range of applications such as gas sensors, magnetic storage media, catalysis,[15,16] batteries, solar energy conversion, high-temperature superconductors,[1,17] and dilute magnetic semiconductors.[12]

The shape, size and structure of material have a great influence on the thermal, chemical and physical properties of the material.[5,15,18] So, reducing the size of the material to nanoscale will give some unique features to the material like homogeneity, large interfacial area, and high surface to volume ratio.[16] The low-cost synthesis of nanostructures has got considerable attention due to their wide range of applications in magnetic, electronic, and photonic devices. The unique structural and dimensional characteristics of them have got its significance in the fabrication of nanoswitches, nanosensors, and transistors.[13] Nowadays, the synthesis of nanomaterials of desired chemical, physical and thermal properties with dimensional control is a challenging goal due to their wide range of practical applications.[13] According to the literature, the morphological variation during the synthesis process highly influences the thermal properties of a material, especially the thermal conductivity. The reports say that the aggregated structure usually gives more thermal conductivity,[19,20] and compared to spherical nanoparticles, nanorods have higher thermal conductivity since the shape factor is high for the nanorods.[19,21]

The low-cost fabrication of nanostructure shapes with desired property monitoring is still a challenging issue. Several methods are possible for the synthesis of CuO with multiple morphologies and shapes. Some of such techniques are the hydrothermal method, sol-gel synthesis, solution-phase chemical synthesis, one-step solid-state reaction technique,[19] and laser ablation technique.[22] Most of these methods require sophisticated equipment, high pressure, temperature, toxic reagents, reducing agents, and electric furnaces.[14,22,23] But the literature reveals that the decomposition of copper hydroxide produces copper oxide even at room temperature in the presence of aqueous media.[13,22,24] Also, this solution-phase decomposition technique has desired mastery over the grain size and shape of the nanoparticles. When the decomposition of copper hydroxide forms copper oxide, the synthesised CuO nanoparticles will show the same morphological characteristics as the parent copper hydroxide. So, the control over the morphological characteristics of the resultant CuO nanoparticles is possible by giving sufficient control on the morphology of the parent copper hydroxide.[19]

The incorporation of nanoparticles into a base fluid

†Corresponding author. E-mail: drssraman@gmail.com
© 2021 Chinese Physical Society and IOP Publishing Ltd

greatly influences the thermal behaviour of the base fluid, making it suitable for heat transfer applications. Among several oxide nanoparticles found to be used in nanofluids, CuO nanoparticles are essential because of their various industrial applications and also as thermal diffusivity enhancers.[1] Since heat transfer occurs at the particle surface, the nanosized particles with a large surface to volume ratio help in improving the heat transfer properties.[25] In layer theory, for a nanofluid, the nanolayer acts as a thermal bridge between the bulk liquid and the solid nanoparticle. Also, the intermediate physical state of the layered molecules between the bulk liquid and solid will increase the thermal conductivity.[26,27] In the case of solids alone, the interfacial resistance between the solid/solid interface will lower the thermal conductivity, which will become a barrier in the heat transfer application. But in particle-liquid suspensions, the contact resistance is not dominant between the solid-liquid interface, which will lead to an enhancement in thermal conductivity.[26,27] The present work reports the variations in the thermal behavior during the formation of CuO from copper hydroxide. The study of thermal diffusivity reveals the changes in the thermal behavior of a sample.

Of several methods-steady-state and non-steady-state-for the thermal characterisation of the material, laser-assisted techniques stand unique in terms of their sensitivity, accuracy, non-destructive nature, and lesser sample requirement for the study.[28,29] The methods such as thermal lens, photo-acoustic, and beam deflection are the popular non-destructive and non-steady state methods for determining the thermal diffusivity of a material.[30–33] In these techniques, only the photons absorbed by the material alone contribute to the photothermal signal that offers a high signal to noise ratio and sensitivity.[29] In this paper, an attempt has been made to unveil the evolution of the thermal behavior of CuO during its formation from $Cu(OH)_2$ by studying the variations in thermal diffusivity using the single beam thermal lens technique.

2. Materials and methods

In the present work, the single beam thermal lens (TL) technique is used to investigate the evolution of thermal diffusivity of CuO nanofluid. In this technique, the same laser source acts as the pump and the probe.[5,34,35] The principle behind the TL spectroscopic technique is the variation of refractive index produced inside the medium due to localized heating through a sufficient laser source.[36] Figure 1 shows the experimental arrangement. A convex lens focuses a He-Cd laser emitting radiations at 442 nm with a power of 80 mW and a focal length of 20 cm on the liquid sample placed inside a cuvette. The continuous wave laser beam is modulated by using an electro-mechanical chopper at a frequency of 4 Hz. The laser beam coming out of the sample is collected by an optical fibre and detected using a sensitive photodiode. The output of the photodiode is displayed using a digital storage oscilloscope (DSO).[37]

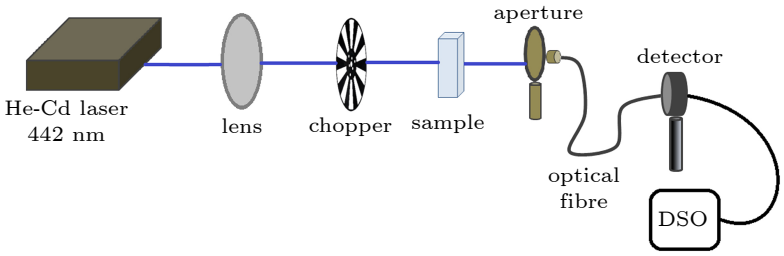


Fig. 1. Schematic representation of single beam thermal lens technique.

The optical absorption resulting in the nonradiative de-excitation develops a temperature gradient inside the sample. Hence, a refractive index gradient occurs within the sample and acts as a concave lens diverging the laser beam. The intensity of the emergent laser beam $I(t)$ is given by[21]

$$I(t) = I(0)\left[1 - \theta\left(1 + \frac{t_c}{2t}\right)^{-1} + \frac{1}{2}\theta^2\left(1 + \frac{t_c}{2t}\right)^{-2}\right]^{-1}, \quad (1)$$

where $I(0)$ is the initial intensity, t_c is the characteristic time constant which is related to the thermal diffusivity (α) and the beam radius (ω) by the relation

$$t_c = \frac{\omega^2}{4\alpha}, \quad (2)$$

and θ is the parameter relating the steady-state intensity, I_∞, and I_0 as given by the equation

$$\theta = 1 - (2I)^{\frac{1}{2}}, \quad (3)$$

where $I = (I_0 - I_\infty)/I_\infty$.

In the present work, 0.5 M copper nitrate ($Cu(NO_3)_2$) and 0.5 M sodium hydroxide (NaOH) are used for the synthesis of copper oxide (CuO) by the chemical precipitation method. For this, NaOH solution is drop wisely added into copper nitrate solution under vigorous stirring at room temperature. After the complete addition of NaOH, 10 ml of the resultant solution is taken and then washed, dried, and ground. This sample is labeled as S1. The same process is repeated at time $t = 4$, 8, 12, 24, 48, 72, and 96 h, and the samples are labeled as S2, S3,

S4, S5, S6, S7, and S8, respectively. The chemical reaction that leads to the generation of CuO[13,14,23,24] is given below:

$$\begin{aligned} \mathrm{Cu(NO_3)_2 + 2NaOH} &\rightarrow \mathrm{Cu(OH)_2 + 2NaNO_3}, \\ \mathrm{Cu(OH)_2} &\rightarrow \mathrm{CuO + H_2O}. \end{aligned} \tag{4}$$

The structural and morphological characterizations of the powdered samples used for preparing the nanofluid are carried out using x-ray diffraction (XRD-Bruker D8 Advanced x-ray diffractometer with Cu $K\alpha$ radiation with a wavelength of 1.5406 Å), Fourier transform infrared (FTIR-Shimadzu IRAffinity-1 FTIR spectrophotometer), and field emission scanning electron microscopy (FESEM-Nova Nano). The UV-visible absorption spectrum is recorded using Jasco-V-550. In the present work, CuO nanofluid is prepared by mixing 1 mg of the sample in 2 ml distilled water, sonicated, and subjected to thermal diffusivity study. C1–C8 are the nanofluids corresponding to the samples S1–S8, respectively.

3. Result and discussion

In the present work, CuO is synthesized at room temperature by the decomposition of the copper hydroxide, produced from copper nitrate and sodium hydroxide. The morphological modification of the reactants transforming into CuO can be understood from the FESEM images of the samples S1–S8 shown in Fig. 2. The FESEM image clearly shows a transformation of rod-like morphology (for S1) into flakes (for S8). Figure 2 reveals that the rod-shaped $Cu(OH)_2$ decomposes into smaller rods during the first eight hours of synthesis (Figs. 2(a)–2(c)). A gradual assembling of smaller rods into flakes takes place up to the 48th hour. After that, a breaking down of the flakes (for S7 and S8) occurs.

The structural characterization of the synthesized sample is carried out by using XRD. The XRD patterns of samples S1–S8 are recorded in the range $2\theta = 15^\circ$ to 80° in a scanning step of 0.02°. We have already investigated and reported[38] the modifications in the XRD pattern during the evolution of $Cu(OH)_2$ to CuO. The XRD pattern shown in Fig. 3 has been reproduced with the permission of the journal, understanding the evolution of CuO. For samples S1–S3, the prominent peaks in the XRD pattern match well with the JCPDS file No. 35-0505, which confirms the orthorhombic structure of copper hydroxide. But, for samples S4–S8, the peaks at 35° and 38° become more intense and sharper, and all the peaks match with the JCPDS file No. 801917 indicating the monoclinic structure of CuO. So, the XRD analysis confirms the transformation of copper hydroxide into copper oxide.

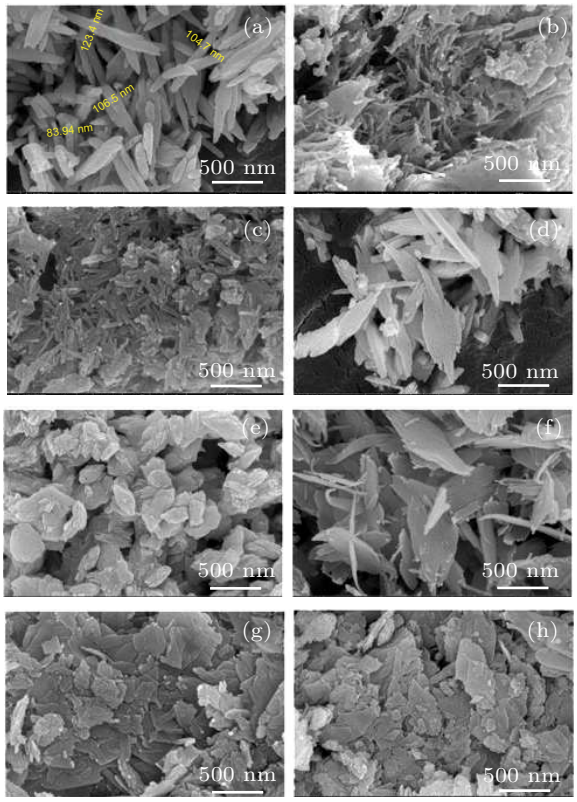


Fig. 2. FESEM images of the samples (a) S1, (b) S2, (c) S3, (d) S4, (e) S5, (f) S6, (g) S7, (h) S8.

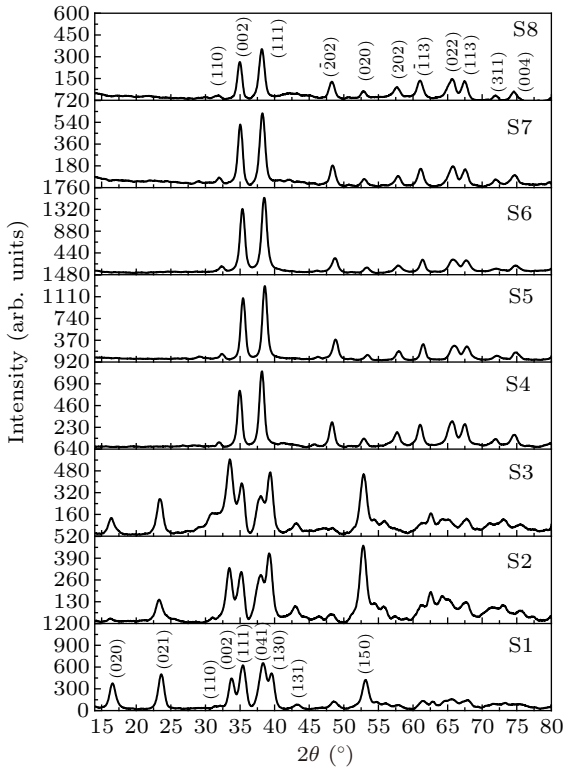


Fig. 3. XRD patterns of samples S1–S8.[38]

The FTIR spectroscopy is another powerful tool for structural characterization where the functional groups present in the material is identified from its frequency of vibration. The FTIR spectrum of the samples S1–S8 is shown in Fig. 4. We

have already reported the modifications in the FTIR spectra during the evolution of CuO from $Cu(OH)_2$.[38] During the transformation of copper hydroxide into copper oxide, in samples S4–S8, the peak around 1050 cm^{-1} due to O–NO_2 stretching vibration disappears, while the peak corresponding to Cu–O stretching mode around 600 cm^{-1} appears. Also, the intensity of peaks due to OH groups, around 830 cm^{-1}, 1350 cm^{-1}, 1640 cm^{-1}, and 3400 cm^{-1}, decreases upon ageing. The study revealed the increase in the intensity of the transmittance peak corresponding to the OH group with time. The presence of the peaks around 600 cm^{-1} and 480 cm^{-1} also suggests the formation of CuO.[39–44]

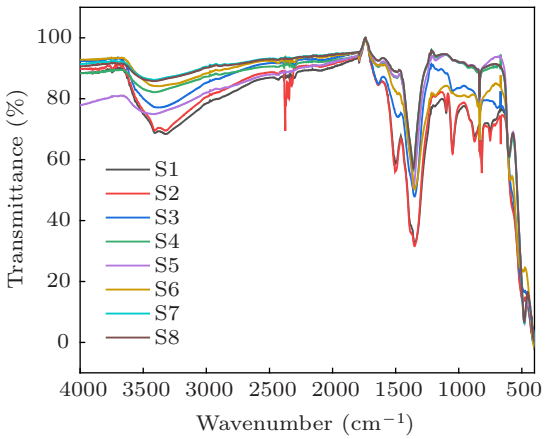


Fig. 4. FTIR spectra of samples S1–S8.

The optical properties of samples C1–C8 are analyzed using the UV-visible absorption spectra, shown in Fig. 5. The figure reveals the enhancement in absorption during the evolution of CuO from copper hydroxide. The UV-visible spectra show an absorption peak around 265 nm due to the charge transfer between 2p orbitals of oxygen and 4s bands of Cu^{2+} ions.[45]

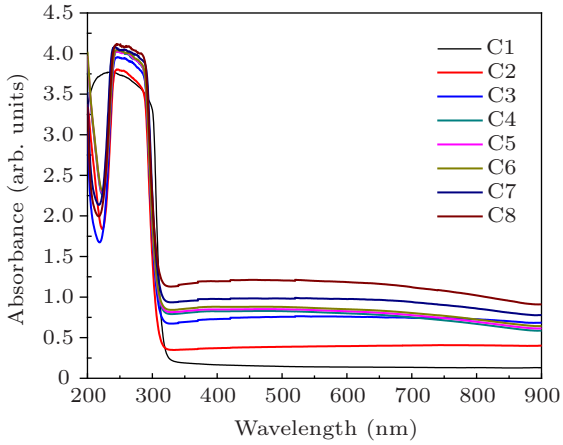


Fig. 5. UV-visible absorption spectra of samples C1–C8.

The chemical decomposition turning $Cu(OH)_2$ into CuO is also reflected by the thermal behavior of the sample. The thermal diffusivity of the CuO nanofluid samples is measured using the single beam thermal lens spectroscopic setup shown in Fig. 1. Single beam thermal lens study helps understand the evolution of thermal diffusivity during the formation of CuO and throws light on the chemical reaction taking place. The formation of the thermal lens within the sample is confirmed by the thermal blooming shown in Fig. 6. The periodic deposition of heat generated by the non-radiative de-excitation develops a temperature gradient inside the medium, which results in thermal blooming. Thermal waves are produced inside the medium with a periodicity same as that of the light falling in the medium. The rings observed in blooming are the result of these thermal waves propagating in the medium. Figure 7(a) shows the output of DSO corresponding to the thermal decay process of sample C4 as a representative, and Fig. 7(b) shows

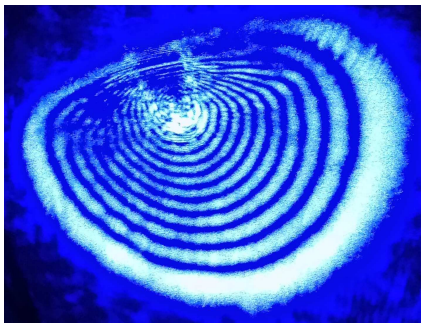


Fig. 6. Thermal blooming.

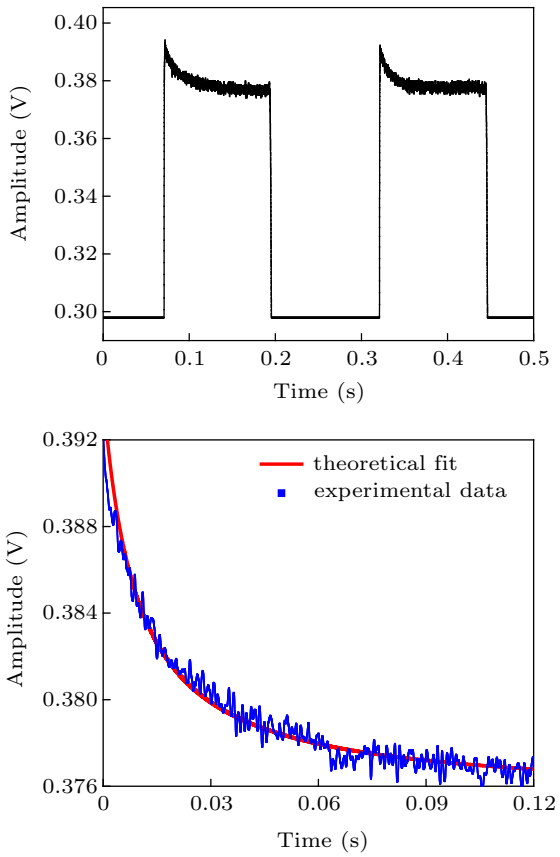


Fig. 7. (a) Thermal lens signals of sample C4 recoded in the DSO. (b) Theoretical fit to the experimental data.

the experimental fit to the decay curve. The refractive index profile of sample C1 is shown in Fig. 8. It can be used to demonstrate the spatial distribution of the refractive index as well as temperature. The change in refractive index will be maximum along the line of propagation of the laser beam.

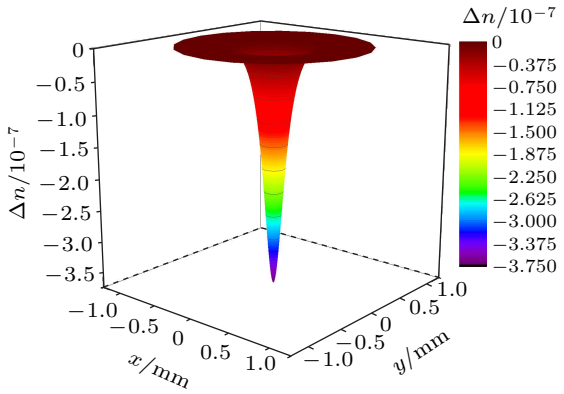


Fig. 8. The spatial variation of refractive index in sample C1.

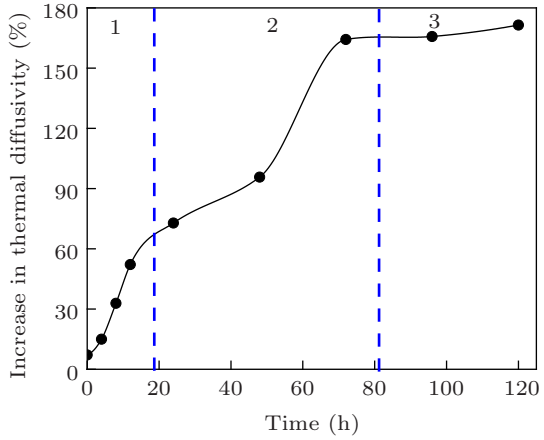


Fig. 9. Variation of thermal diffusivity of CuO with ageing.

The thermal diffusivity of different samples is calculated using Eq. (2). From the variation of thermal diffusivity with time shown in Fig. 9, it is evident that the decomposition rate or the reaction rate is high during the initial stage and slows down later. Accordingly, Fig. 9 can be divided into three regions. In region 3, the XRD (Fig. 3) and FTIR analysis has confirmed that the system contains CuO. The near stopping of chemical decomposition appears as a reduction in the rate of change of thermal diffusivity, as shown in Fig. 10. Though the thermal diffusivity increases during the transformation of $Cu(OH)_2$ into CuO, the variation in its rate of change indirectly points to the reaction kinetics. In other words, the thermal lens study helps not only in understanding the evolution of thermal diffusivity of material during its formation but also reveals the reaction dynamics involved. The enhancement of thermal diffusivity of the base fluid (here, water) is 165% towards the end of the decomposition reaction when CuO is formed. The increase in the thermal diffusivity value depends significantly on the morphological modifications displayed in Fig. 2. An observation through Figs. 2(a)–2(h) indicates morphological modification from a more porous to a less porous system as a result of the aggregation of nanorods into flakes. This brings in reduced phonon scattering resulting in thermal diffusivity enhancement. The experimental results reveal that as the amount of OH group decreases, the thermal diffusivity value increases.

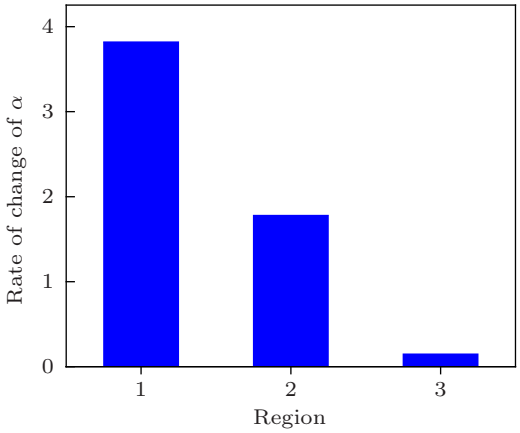


Fig. 10. Rate of change of thermal diffusivity (α) at the three regions.

4. Conclusion

The paper reports the evolution of thermal diffusivity during the formation of material, taking CuO as an example. The single-beam TL technique can be used for the TL study of the decomposition of $Cu(OH)_2$ into CuO due to ageing. The morphological modification is analyzed from the FESEM images. The structural analysis carried out using the XRD and FTIR confirms the transformation into CuO. The UV-visible spectroscopic study shows an increase in absorption during the process of evolution. The thermal diffusivity study carried out at different stages during the ageing process indicates three steps. In the initial one, the rate of increase of thermal diffusivity value is attributed to the faster rate of chemical transformation, which slows down in subsequent stages. The study shows that the thermal diffusivity enhancement of the base fluid is 165% when CuO has formed. The reason for this increase in the thermal diffusivity value is evidenced by the morphological modifications taking place as a result of the aggregation of smaller nanorods into larger flakes resulting in the reduction of phonon scattering. Besides the morphological modifications, the variation in the number of hydroxyl groups in the sample is also found to influence the thermal diffusivity significantly. Thus, the study points to the dynamics of thermal diffusivity evolution in copper oxide nanofluid.

References

[1] Dey K K, Kumar A, Shanker R, Dhawan A, Wan M, Yadav R R and Srivastava A K 2012 *RSC Adv.* **2** 1387
[2] Gupta V, Magotra U, Sharma A K and Sharma M 2020 *Russ. J. Phys. Chem. A* **94** 2312

[3] Yu W, Xie H, Chen L and Li Y 2009 *Thermochim. Acta* **491** 92
[4] Shima P D, Philip J and Raj B 2010 *J. Phys. Chem. C* **114** 18825
[5] Sebastian R, Swapna M S, Raj V, Hari M and Sankararaman S 2018 *Mater. Res. Express* **5** 75001
[6] Sekhar T V R, Nandan G, Prakash R and Muthuraman M 2018 *Mater. Today Proc.* **5** 6176
[7] Suresh T, Uthayakumar G and Srinivasan R 2016 *International Conference on Energy Efficient Technologies for Sustainability (ICEETS)* (IEEE) p. 202
[8] Das S K, Putra N, Thiesen P and Roetzel W 2003 *J. Heat Transf.* **125** 567
[9] Sultana J, Das A, Das A, Saha N R, Karmakar A and Chattopadhyay S 2016 *Thin Solid Films* **612** 331
[10] Masudy-Panah S, Siavash Moakhar R, Chua C S, Tan H R, Wong T I, Chi D and Dalapati G K 2016 *ACS Appl. Mater. Interfaces* **8** 1206
[11] Jin Z, Zhang X, Li Y, Li S and Lu G 2007 *Catal. Commun.* **8** 1267
[12] Sekhar H, Kumar Y R and Rao D N 2015 *Observation of Confinement Effects through Liner and Nonlinear Absorption Spectroscopy in Cuprous oxide IOP Conference Series: Materials Science and Engineering* (Vol. 73) (IOP Publishing) p. 12078
[13] Wang W, Wang L, Shi H and Liang Y 2012 *Cryst. Eng. Comm.* **14** 5914
[14] Anandan S, Wen X and Yang S 2005 *Mater. Chem. Phys.* **93** 35
[15] Zheng L and Liu X 2007 *Mater. Lett.* **61** 2222
[16] Hong Z, Cao Y and Deng J 2002 *Mater. Lett.* **52** 34
[17] Das D, Nath B C, Phukon P and Dolui S K 2013 *Colloids Surfaces B Biointerfaces* **101** 430
[18] Sebastian R, Swapna M S and Sankararaman S 2020 *TSN Appl. Sci.* **2** 1
[19] Prasher R, Phelan P E and Bhattacharya P 2006 *Nano Lett.* **6** 1529
[20] Wang B X, Zhou L P and Peng X F 2003 *Int. J. Heat Mass Transf.* **46** 2665
[21] Hari M, Joseph S A, Mathew S, Nithyaja B, Nampoori V P N and Radhakrishnan P 2013 *Int. J. Therm. Sci.* **64** 188
[22] Bhosale M A, Karekar S C and Bhanage B M 2016 *ChemistrySelect* **1** 6297
[23] Chen K and Xue D 2013 *J. Phys. Chem. C* **117** 22576
[24] Cudennec Y and Lecerf A 2003 *Solid state Sci.* **5** 1471
[25] Lee S, Choi S-S, Li and S and Eastman J A 1999 *J. Heat Transfer* **121** 280
[26] Yu W and Choi S U S 2004 *J. Nanoparticle Res.* **6** 355
[27] Yu W and Choi S U S 2003 *J. Nanoparticle Res.* **5** 167
[28] Bindhu C V, Harilal S S, Nampoori V P N and Vallabhan C P G 1998 *Optical Engineering* **37** 2791
[29] Sanakara Raman S 1999 *Investigation on thermal diffusivity of some selected materials using laser induced photoacoustic technique* (Ph. D. thesis) (Kerala: International School of Photonics, Cochin University of Science and Technology)
[30] Sankara Raman S, Nampoori V P N, Vallabhan C P G, Ambadas G and Sugunan S 1999 *J. Appl. Phys.* **85** 1987
[31] Sankara Raman S, Nampoori V P N, Vallabhan C P G, Ambadas G and Sugunan S 1995 *Appl. Phys. Lett.* **67** 2939
[32] Havaux M, Lorrain L and Leblanc R M 1990 *Photosynth. Res.* **24** 63
[33] Ghizoni C C and Miranda L C M 1985 *Phys. Rev. B* **32** 8392
[34] Swapna M S, Manjusha S, Raj V, Hari M and Sankararaman S 2018 *JOSA B* **35** 1662
[35] Raj V, Soumya S, Swapna M S and Sankararaman S 2018 *Mater. Res. Express* **5** 115504
[36] Navas M J and Jimenez A M 2003 *Crit. Rev. Anal. Chem.* **33** 77
[37] Mahdieh M H and Akbari Jafarabadi M 2012 *Opt. Laser Technol.* **44** 78
[38] Sebastian R, Swapna M S, Devi H V saritha, Raj V, Hari M and Sankararaman S 2019 *Mater. Res. Express* **6** 116202
[39] Liu Y, Ren W and Cui H 2011 *Micro. Nano. Lett.* **6** 823
[40] Li C, Yin Y, Hou H, Fan N, Yuan F, Shi Y and Meng Q 2010 *Solid State Commun.* **150** 585
[41] Prakash V and Diwan R K 2015 *Indian J. Pure Appl. Phys.* **53** 753
[42] Shahmiri M, Ibrahim N A, Shayesteh F, Asim N and Motallebi N 2013 *J. Mater. Res.* **28** 3109
[43] Zhang Y X, Huang M, Li F and Wen Z Q 2013 *Int. J. Electrochem. Sci.* **8** 8645
[44] Zhang L, Lu W, Feng Y, Ni J, Lü Y and Shang X 2008 *Acta Physico-Chimica Sin.* **24** 2257
[45] Nath A and Khare A 2011 *J. Appl. Phys.* **110** 43111